

# Broadband Axion Dark Matter Haloscopes via Electric Field Sensing

Ben T. McAllister,<sup>1,\*</sup> Maxim Goryachev,<sup>1</sup> Jeremy Bourhill,<sup>1</sup> Eugene N. Ivanov,<sup>1</sup> and Michael E. Tobar<sup>1,†</sup>

<sup>1</sup>*ARC Centre of Excellence For Engineered Quantum Systems,  
Department of Physics, School of Physics and Mathematics,  
University of Western Australia, 35 Stirling Highway, Crawley WA 6009, Australia.*  
(Dated: June 15, 2022)

The mass of axion dark matter is only weakly bounded by cosmological observations, necessitating a variety of detection techniques and experiments at many different mass ranges. Axions are expected to couple to photons via the inverse Primakoff effect and cryogenic resonant cavities are often proposed as a tool for detecting these photons. However, such structures are inherently narrowband and the range of possible axion dark matter masses spans several orders of magnitude. On the other hand broadband low-mass particle haloscopes have been proposed using inductive magnetometer sensors coupled to SQUID amplifiers and requiring a solenoid magnet of gapped toroidal geometry. In this work we propose an alternative approach, which uses a capacitive sensor in a conventional solenoidal magnet with the magnetic field aligned in the laboratory z-axis, as implemented in standard haloscope experiments. In the presence of a large DC magnetic field, the inverse Primakoff effect causes a time varying electric field (or displacement current) in the z-direction to oscillate at the axion Compton frequency. We propose non-resonant techniques to detect this electric field by implementing capacitive sensors coupled to a low noise amplifier. We present the theoretical foundation for this proposal, and the first experimental results. Preliminary results constrain  $g_{a\gamma\gamma} > \sim 2.35 \times 10^{-12} \text{ GeV}^{-1}$  in the mass range of  $2.08 \times 10^{-11}$  to  $2.2 \times 10^{-11}$  eV, and demonstrate potential sensitivity to axion like dark matter with masses in the range of  $10^{-12}$  to  $10^{-8}$  eV.

## INTRODUCTION

For decades now numerous cosmological observations have suggested the presence of a large amount of excess matter in the universe, of unknown composition [1, 2]. The lack of direct observation of this matter suggests that it is only very weakly-interacting with the standard model particles, particularly photons. For these reasons it is often dubbed “dark” matter. Some suggest that these cosmological observations may be accounted for by modifying the laws of gravity, but by far the most well motivated and explored theories are those that propose new particles. Many types of new particles are often proposed over a vast mass range (from sub-eV to GeV). Consequently we need a large number of experiments at different mass scales, and preferably broadband experiments. Recent cosmological evidence combined with the null results of many large experiments points away from the traditional WIMP hypotheses, and towards the low-mass regime [3–5]. This work will focus on a theoretical (sub-eV mass) particle known as the axion, as well as other axion-like particles (ALPs).

## AXIONS

Axions are hypothetical neutral, spin zero bosons often proposed as an elegant solution to the strong charge-parity problem in quantum chromodynamics [6, 7]. They are a type of weakly interacting slim particle [8], which is a class of particles of increasing promise to comprise dark matter. Axions and ALPs can be formulated as a

primary component of the dark matter [9].

If axions or ALPs do comprise the majority of dark matter, there should be an abundance of such particles in the laboratory frame on earth, and thus laboratory experiments may detect the presence of axions. Perhaps the most often explored ALP to standard model coupling is via the inverse Primakoff effect. In this coupling, an axion interacts with a photon (usually in an experiment this is a virtual photon supplied by a DC magnetic field) and converts into a second, real photon such that

$$\hbar\omega_a \approx m_a c^2 + \frac{1}{2}m_a v_a^2,$$

where  $m_a$  is the mass of the axion,  $\omega_a$  is the frequency of the generated real photon,  $\hbar$  is the reduced Planck’s constant,  $c$  is the speed of light, and  $v_a$  is the velocity of the axion with respect to the laboratory frame, the distribution of axion velocities with respect to earth gives a “line-width” or effective quality factor for the axion signal of approximately  $10^6$  [10, 11]. The strength of this axion-photon interaction, and the mass of the axion are given by,

$$g_{a\gamma\gamma} = \frac{g_\gamma \alpha}{f_a \pi}, \quad m_a = \frac{z^{1/2}}{1+z} \frac{f_\pi m_\pi}{f_a}.$$

Here  $z$  is the ratio of up and down quark masses,  $\frac{m_u}{m_d} \approx 0.56$ ,  $f_\pi$  is the pion decay constant  $\approx 93$  MeV,  $m_\pi$  is the neutral pion mass  $\approx 135$  MeV,  $g_\gamma$  is an axion-model dependent parameter of order 1, and  $\alpha$  is the fine structure constant [12–16]. Confounding experimental efforts to detect axions via this coupling is the fact that  $f_a$ , the Peccei-Quinn Symmetry Breaking Scale, is unknown,

and hence both the mass and strength of axion-photon coupling are unknown. This means that both the location in frequency space and the expected amplitude of any axion induced signals are unknown, although we do have some broad limits from cosmological observations and previous experiments [17, 18]. There are theoretical predictions for axions over a wide range of masses, and a host of experiments and proposals exploring both high and low masses [19–29].

Typically experiments that attempt to exploit the Primakoff coupling rely on a tunable resonant structure designed to capture and detect the photons generated by axion conversion. The specific design of these resonant systems depends heavily on the axion mass range in question, but most dark matter axion detection experiments operate in the microwave and millimeter-wave regimes. These experiments are inherently narrowband, which is a limitation, as the axion mass and therefore the corresponding photon frequency is unknown.

More recently ABRACADABRA was proposed, which is partly a broadband low-mass particle haloscope [26] designed to detect the photons generated by low mass, pre-inflationary dark matter axions. This experiment uses a solenoid magnet of gapped toroidal geometry and via the inverse Primakoff effect produces an oscillating magnetic field at the Compton frequency in the laboratory  $z$ -direction. The oscillating magnetic field is detected by an inductive magnetometer sensor coil coupled to a SQUID amplifier. In contrast, we propose a technique that may be implemented in the same setup as a standard resonant haloscope with a conventional solenoidal DC magnetic field aligned in the  $z$ -direction. It is well known in this setup that the inverse Primakoff effect induces a time varying electric field (or displacement current) in the same direction as the magnetic field, which oscillates at the axion Compton frequency. We propose non-resonant techniques to detect this electric field by considering capacitive sensors coupled to low noise current and voltage amplifiers. We name this experiment: Broadband Electric-field Axion Sensing Technique or BEAST. This proposal bears some similarities to an inductive, low-mass axion detection proposal [28], but this work relies on capacitive sensing and is broadband, rather than resonant. In order to derive the axion-modified Maxwell's equations, we begin with the Lagrangian for axions coupled to photons

$$\mathcal{L} = \frac{1}{2}(\partial_\mu a)^2 - \frac{1}{2}m_a^2 a^2 - \frac{1}{4}F_{\mu\nu}F^{\mu\nu} + \frac{1}{4}g_{a\gamma\gamma}aF_{\mu\nu}\tilde{F}^{\mu\nu}.$$

From this it can be shown that we arrive at the modified

Maxwell's equations (in SI units, in media) [30],

$$\begin{aligned}\epsilon_r \vec{\nabla} \cdot \vec{E} &= \frac{\rho}{\epsilon_0} + g_{a\gamma\gamma}c\vec{B} \cdot \nabla a, \\ \frac{1}{\mu_r} \vec{\nabla} \times \vec{B} - \frac{1}{c^2}\epsilon_r \frac{\partial \vec{E}}{\partial t} &= \mu_0 \vec{J} - \frac{g_{a\gamma\gamma}}{c} \left( \vec{B} \frac{\partial a}{\partial t} + \nabla a \times \vec{E} \right), \\ \vec{\nabla} \cdot \vec{B} &= 0, \\ \vec{\nabla} \times \vec{E} &= -\frac{\partial \vec{B}}{\partial t}.\end{aligned}$$

Here  $\vec{E}$  is electric field,  $\rho$  is charge density,  $\epsilon_r$  and  $\epsilon_0$  are the relative and vacuum permittivity,  $\vec{B}$  is magnetic field,  $a$  is the axion scalar field,  $\mu_r$  and  $\mu_0$  are the relative and vacuum permeability,  $c$  is the speed of light in vacuum, and  $\vec{J}$  is current density. It is worth noting that all terms containing  $g_{a\gamma\gamma}$  are often presented with the opposite sign, but it has no impact on this work. With these relationships we can find the RF electric and magnetic fields induced by axion conversion inside a cylindrical solenoidal magnetic field ( $\vec{B} = B_0\hat{z}$ ). These are given by [31],

$$\begin{aligned}\vec{E}_a &= E_a\hat{z} = \frac{1}{\epsilon_r}g_{a\gamma\gamma}cB_0a\hat{z}, \\ \vec{B}_a &= \mu_r \frac{1}{2} \frac{g_{a\gamma\gamma}}{c} r B_0 \frac{\partial a}{\partial t} \hat{\phi}.\end{aligned}$$

Here  $r$  is the distance from the centre of the solenoid, and  $\hat{z}$  and  $\hat{\phi}$  are the  $z$ -direction and  $\phi$ -direction unit vectors in the cylindrical co-ordinate system of the solenoid.

## CAPACITIVE SENSING

### A Simple Parallel Plate Capacitor

In this section we consider the detection of the electric field produced by the inverse Primakoff effect by monitoring the signal from a parallel plate capacitor embedded in the magnetic field, such that the vector area of the plates are aligned with the induced electric field. From the modified Maxwell's equations the expected voltage and current output from such a capacitor due to Primakoff axion conversion can be derived. The capacitance of a parallel plate capacitor with plate area  $A$  and separation  $d$  is given by  $C = \frac{\epsilon_0\epsilon_r A}{d}$ . The voltage across the plates as a result of the axion induced electric field,  $\vec{E}_a$  is given by

$$V = \int_0^d E_a dz = \frac{1}{\epsilon_r}g_{a\gamma\gamma}cB_0ad,$$

where  $a = a_0 \cos(\omega_a t)$  and  $a_0 = \sqrt{\frac{2\rho_a}{c} \frac{\hbar}{m_a}}$  [32]. We can now derive (see appendix),

$$\begin{aligned}I_{a_{RMS}} &= -g_{a\gamma\gamma}\epsilon_0 AB_0 \sqrt{\rho_a c^5} \\ V_{a_{RMS}} &= \frac{1}{\epsilon_r}g_{a\gamma\gamma}B_0 \sqrt{\rho_a c^5} \frac{1}{\omega_a} d.\end{aligned}\tag{1}$$

Interestingly, neither the capacitor plate separation nor the permittivity of the material between the plates has an impact on the current we expect, as these factors cancel out of the above expressions- however, the area of the capacitor plates is an important factor. Conversely, the voltage across the plates depends only on the permittivity and the plate separation, not the area. An optimal detector for such an experiment thus depends on the method of readout. If we wish to read current with, for example, a SQUID, we would implement the largest diameter capacitors that would fit inside the magnet bore. If we were to read voltage directly with, for example, a high-impedance amplifier, we would design for the lowest permittivity and largest plate separation achievable. However, one must be mindful that the derivation assumes an ideal parallel plate structure, with no fringing or parasitic capacitance.

### Beyond a Simple Parallel Plate Capacitor

When compared with a resonant experiment such as a typical haloscope, the trade-off is that we lose the resonant enhancement of the signal by the quality factor of the resonance ( $Q$ ). However, in principal it is possible to combine the signals from many capacitors in the same magnetic field to enhance our sensitivity. Typical microwave  $Q$ s in axion haloscopes are on the order of  $10^4$  to  $10^5$ , and whilst it is unlikely that combining this many capacitors inside a single magnet bore would be readily achievable, it should be possible to install 10s, 100s, or perhaps (with specialized machining and manufacturing) 1000s of capacitors inside a cylindrical magnet bore. The optimal strategy for this capacitor combination depends on the method of readout, and various other limitations such as stray capacitance.

For example, in a voltage readout we note that the plate area is unimportant and may thus opt for a number of very small diameter capacitors with large plate separations, inside a single magnetic field. In such a case, to avoid issues associated with having very small plate areas with very large plate separations we may instead opt to combine many small capacitors (small plate area and small plate separation) in series to create a “chain” of capacitors, with an effective total plate separation equal to the sum of the plate separations in the chain. This would maintain large effective plate separations, whilst simultaneously allowing for very low plate areas, and thus allowing for many such chains inside the same magnet. To understand how a scheme like this would work, cross capacitance between each element and stray capacitance due the experimental chamber and grounding would need to be modelled carefully.

In contrast, for the current readout scheme, large plate areas are required with arbitrary plate separations. In such a scheme it would be optimal to create many thin

parallel capacitors with large plate area and then combine the current outputs. Again placement within the magnet bore and the avoidance of stray capacitances or accidental electrical connection of neighbouring capacitors would need to be carefully considered.

Another prospect would be to sense the electric field with an array of long wire dipole antennas aligned along the z-axis and combine the outputs. Oscillating current in the wires would be driven by the oscillating electric field induced by the axion and these currents could be combined. The capacitance and frequency response of such structures are well known, and they are generally broadband with a low frequency cutoff and a high frequency resonance. Such techniques may be suitable in a different mass range to that proposed in this work.

Finally, we propose an axion haloscope sensitive to low-mass axions, where a number of capacitors are coupled to a low noise amplifier such as a SQUID or other device (such as a high impedance amplifier), inside a static magnetic field. The output of the amplifier may then be measured, and used to detect or exclude axions. This measurement is broadband, and is thus sensitive to axions over a wide range of mass values simultaneously. The bandwidth of the amplifier sets the limit on the mass range achievable in such a search. For example, in the case of a SQUID readout the location of the resonance which will be generated by the combination of the capacitor and SQUID input inductor (which will occur at a few MHz for commercial capacitor values) will be the limiting factor.

### SENSITIVITY ESTIMATES

We now discuss projected sensitivities for the experiments discussed above, with two readout schemes presented.

#### SQUID current readout

It has previously been found that SQUIDs can detect RMS current spectral densities on the order of  $0.5 \frac{pA}{\sqrt{Hz}}$  within reasonable time frames [33]. The peak of the spectral density of the RMS axion-induced current from the capacitor can be approximated by

$$\frac{I_{a_{RMS}}}{\sqrt{\pi \times BW}}, \quad (2)$$

where  $BW$  is the bandwidth of the axion signal, roughly  $10^{-6}$  times the central frequency.

We can combine equations (1) and (2) and compare with the minimum detection threshold of  $0.5 \frac{pA}{\sqrt{Hz}}$  to find the smallest possible  $g_{a\gamma\gamma}$  detectable with such a setup as a function of axion mass. For general parameters this is

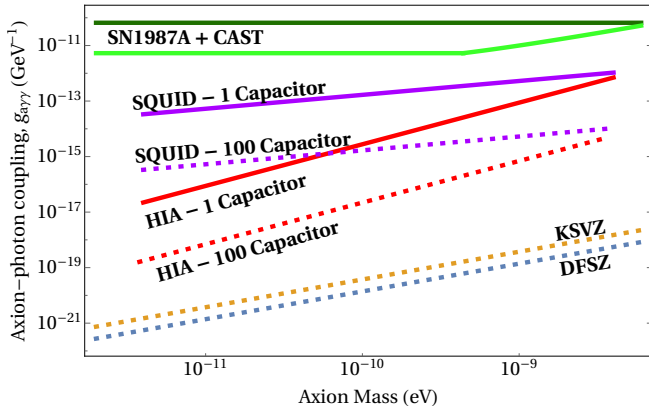


FIG. 1: Projected limits for the BEAST experiment, utilizing: a single capacitor (purple) and 100 capacitors (purple, dashed) coupled to a SQUID, and a single capacitor (red) and 100 capacitors (red, dashed) coupled to a high-impedance amplifier. Current best limits in the region from CAST (green) SN1987A (light green) are also plotted. Also shown are popular axion model bands, KSVZ (gold, dashed) and DFSZ (blue, dashed).

given by,

$$g_{a\gamma\gamma} = \frac{5.2 \times 10^{-20} \sqrt{m}}{AB\sqrt{\rho}}.$$

With  $m$  in eV, and everything else in SI units we obtain  $g_{a\gamma\gamma}$  in  $\text{GeV}^{-1}$ . Figure 1 shows projected limits for 10 cm diameter capacitors embedded in a 14 T magnetic field, coupled to SQUIDS, with arbitrary plate separation and an arbitrary material between the plates, assuming that the dark matter is comprised of axions with an energy density of  $0.45 \frac{\text{GeV}}{\text{cm}^3}$ .

### High-impedance amplifier voltage readout

If we instead decide to read out capacitor voltage directly, employing a high-impedance amplifier, we can follow a very similar process to estimate sensitivity. The effective total voltage noise referred to the input of high-impedance amplifiers depends on a number of factors, but for the purposes of this estimate we use a value of  $100 \frac{nV}{\sqrt{Hz}}$  (see appendix for calculations). Defining the peak spectral density of the RMS axion-induced voltage from the capacitor in the same way as for the current, we can arrive at the projected exclusion limits in much the same way. In this case we compare the peak of the axion-induced rms-voltage PSD with the above voltage noise. For general parameters we arrive at,

$$g_{a\gamma\gamma} = \frac{4.4 \times 10^{-10} m^{3/2} \epsilon_r}{Bd\sqrt{\rho}}.$$

With  $m$  in eV, and everything else in SI units we obtain  $g_{a\gamma\gamma}$  in  $\text{GeV}^{-1}$ . Figure 1 also shows projected limits

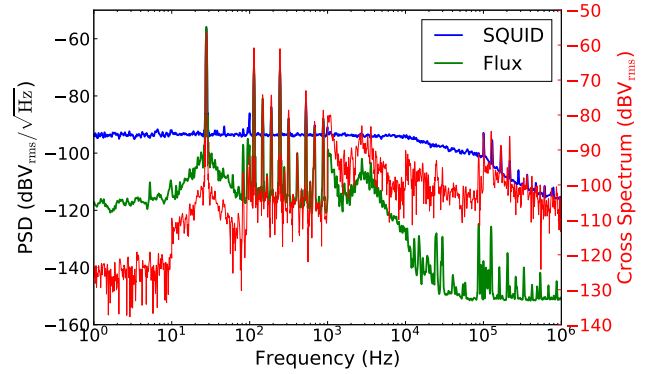


FIG. 2: Observed voltage noise spectra at the output of the SQUID in the first run of BEAST. The blue (green) trace corresponds to the SQUID (flux) line, whilst the red trace corresponds to the cross-spectrum.

for capacitors (or chains of capacitors) with a net effective plate separation of 0.4 m, with vacuum between the plates, and assuming again that the dark matter is comprised of axions with an energy density of  $0.45 \frac{\text{GeV}}{\text{cm}^3}$ .

### FIRST EXPERIMENT WITH A SIMPLE PARALLEL PLATE CAPACITOR

The first BEAST experiment, which searches for low-mass axions consists of a simple parallel plate capacitor coupled to a SQUID amplifier. In this experiment a  $7.5 \times 7$  cm rectangular capacitor was embedded in a 7 T magnetic field at 4 K for 8 days of observation time. The capacitor was coupled to a SQUID with a -3 dB bandwidth of 2.1 MHz and a transimpedance of 1.2 M $\Omega$ .

Figure 2 shows the spectra obtained up to 1 MHz. This illustrates the abundance of spurious signals in this region. However, it is possible to discriminate against these signals with the use of the flux line, which is susceptible to spurious RF signals in the laboratory. This wide span search does not have the requisite spectral resolution to resolve axion signals with an effective linewidth of  $10^{-6} \times \omega_a$ , but serves to demonstrate the expected output spectrum of such an experiment, and highlight the issue of spurious noise sources.

A higher-resolution search was conducted in the region around 5 kHz, with the minimal spectral resolution of 4.5 mHz (increasing at higher frequencies), thus providing the requisite spectral resolution to detect narrow ALP signals. All sharp peaks greater than  $\sim 4.4$  standard deviations from the mean originating from the SQUID were able to be excluded, due to a similar signal appearing in the flux line, as shown in figure 2. Using this data, we may place the 95 % confidence exclusion limits on axion-photon coupling shown in figure 3. The average level of these limits is  $g_{a\gamma\gamma} > \sim 2.35 \times 10^{-12}$ , with some varia-

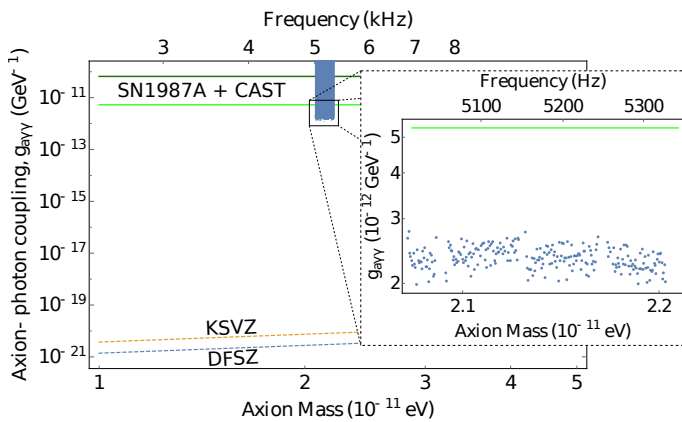


FIG. 3: Exclusion limits from the proof of concept experiment with a single capacitor coupled to a SQUID. Previous best limits in the region from CAST (green) SN1987A (light green) are also plotted. Also shown are popular axion model bands, KSVZ (gold, dashed) and DFSZ (blue, dashed). The inset shows the actual limit as a function of mass, including the narrow regions where limits could not be placed due to large noise sources.

tion as a function of mass. This experiment serves as a brief, narrowband proof of concept, and can be readily extended to wider mass ranges.

### FUTURE SEARCHES

In conjunction with the planned ORGAN experiment [25] at high axion masses, we are developing a capacitive sensing-based experiment for low-mass searches which may run in parallel with the traditional haloscope, utilizing the extra space in the 14 T magnet bore. Technical limitations with availability of equipment, data acquisition and processing prevented a wider search from being feasible within the time scale of this first experiment, however in the future a dedicated system will be built and FPGA-based solutions to data acquisition issues will be implemented.

It is worth noting that if we were to employ a direct voltage readout via a high-impedance amplifier, we would not necessarily need to conduct the experiment cryogenically, as the noise floors of these devices are exceptionally low, even at room temperature. Rare-earth magnets are capable of achieving magnetic fields on the order of a Tesla and, unlike superconducting solenoids, require no cryogenic environment to operate. Although these fields are considerably lower than those achievable with superconducting solenoids, an experiment could be conducted on a bench-top, without the need of a dedicated cryogenic cooler or magnet, and could thus operate continuously for very long times, mitigating to some extent the reduced

sensitivity associated with a lower magnetic field.

### CONCLUSION

We propose a promising broadband (non-resonant) experiment to detect low-mass dark matter axions or ALPs, exploiting the axion-photon coupling via the inverse Primakoff effect. In this proposal a capacitive electric field sensor is placed inside a strong magnetic field, and the electric field generated by axion-photon conversion may be detected via the readout of the sensor, which is coupled to a SQUID or other amplifier. Contrary to most traditional haloscopes the proposed experiment is inherently broadband, which is advantageous for axion detection given that the axion mass is unknown. The sensitivity, limitations and prospects of this technique are discussed, and the exclusion limits from an initial experiment are presented, which exceed the best current limits in the region.

This work was funded by Australian Research Council (ARC) grant No. CE170100009, the Australian Government's Research Training Program, and the Bruce and Betty Green Foundation.

\* ben.mcallister@uwa.edu.au

† michael.tobar@uwa.edu.au

- [1] V. C. Rubin, W. K. Ford, Jr., and N. Thonnard, *Astrophys. J.* **238**, 471 (1980).
- [2] M. Markevitch, A. H. Gonzalez, D. Clowe, A. Vikhlinin, W. Forman, C. Jones, S. Murray, and W. Tucker, *Astrophys. J.* **606**, 819 (2004), astro-ph/0309303.
- [3] R. Barkana, *Nature*, **555**, 71 (2018).
- [4] J. D. Bowman, A. E. E. Rogers, R. A. Monsalve, T. J. Mozdzen, and N. Mahesh, *Nature*, **555**, 67 (2018).
- [5] E. Aprile, J. Aalbers, F. Agostini, M. Alfonsi, F. D. Amaro, M. Anthony, F. Arneodo, P. Barrow, L. Baudis, B. Bauermeister, M. L. Benabderrahmane, T. Berger, P. A. Breur, A. Brown, A. Brown, E. Brown, S. Bruenner, G. Bruno, R. Budnik, L. Bütikofer, J. Calvén, J. M. R. Cardoso, M. Cervantes, D. Cichon, D. Coderre, A. P. Colijn, J. Conrad, J. P. Cussonneau, M. P. Decowski, P. de Perio, P. Di Gangi, A. Di Giovanni, S. Diglio, G. Eurin, J. Fei, A. D. Ferella, A. Fieguth, W. Fulgione, A. Gallo Rosso, M. Galloway, F. Gao, M. Garbini, R. Gardner, C. Geis, L. W. Goetzke, L. Grandi, Z. Greene, C. Grignon, C. Hasterok, E. Hogenbirk, J. Howlett, R. Itay, B. Kaminsky, S. Kazama, G. Kessler, A. Kish, H. Landsman, R. F. Lang, D. Lellouch, L. Levinson, Q. Lin, S. Lindemann, M. Lindner, F. Lombardi, J. A. M. Lopes, A. Manfredini, I. Maris, T. Marrodán Undagoitia, J. Masbou, F. V. Massoli, D. Masson, D. Mayani, M. Messina, K. Micheneau, A. Molinari, K. Mora, M. Murra, J. Naganoma, K. Ni, U. Oberlack, P. Pakarha, B. Pelssers, R. Persiani, F. Piastra, J. Pienaar, V. Pizzella, M.-C. Piro, G. Plante, N. Priel,

- L. Rauch, S. Reichard, C. Reuter, B. Riedel, A. Rizzo, S. Rosendahl, N. Rupp, R. Saldanha, J. M. F. dos Santos, G. Sartorelli, M. Scheibelhut, S. Schindler, J. Schreiner, M. Schumann, L. Scotto Lavina, M. Selvi, P. Shagin, E. Shockley, M. Silva, H. Simgen, M. v. Sivers, A. Stein, S. Thapa, D. Thers, A. Tiseni, G. Trincherro, C. Tunnell, M. Vargas, N. Upole, H. Wang, Z. Wang, Y. Wei, C. Weinheimer, J. Wulf, J. Ye, Y. Zhang, and T. Zhu (XENON Collaboration), *Phys. Rev. Lett.* **119**, 181301 (2017).
- [6] R. D. Peccei and H. R. Quinn, *Phys. Rev. Lett.* **38**, 1440 (1977).
- [7] F. Wilczek, *Phys. Rev. Lett.* **40**, 279 (1978).
- [8] J. Jaeckel and A. Ringwald, *Annual Review of Nuclear and Particle Science* **60**, 405 (2010).
- [9] J. Ipser and P. Sikivie, *Phys. Rev. Lett.* **50**, 925 (1983).
- [10] P. Sikivie, *Phys. Rev. Lett.* **51**, 1415 (1983).
- [11] P. Sikivie, *Phys. Rev. D* **32**, 2988 (1985).
- [12] J. E. Kim, *Phys. Rev. Lett.* **43**, 103 (1979).
- [13] J. E. Kim and G. Carosi, *Rev. Mod. Phys.* **82**, 557 (2010).
- [14] M. Dine, W. Fischler, and M. Srednicki, *Physics Letters B* **104**, 199 (1981).
- [15] M. Shifman, A. Vainshtein, and V. Zakharov, *Nuclear Physics B* **166**, 493 (1980).
- [16] M. Dine and W. Fischler, *Physics Letters B* **120**, 137 (1983).
- [17] L. Abbott and P. Sikivie, *Physics Letters B* **120**, 133 (1983).
- [18] J. Preskill, M. B. Wise, and F. Wilczek, *Physics Letters B* **120**, 127 (1983).
- [19] G. Ballesteros, J. Redondo, A. Ringwald, and C. Tamarit, *Phys. Rev. Lett.* **118**, 071802 (2017), arXiv:1608.05414 [hep-ph].
- [20] S. J. Asztalos, G. Carosi, C. Hagmann, D. Kinion, K. van Bibber, M. Hotz, L. J. Rosenberg, G. Rybka, J. Hoskins, J. Hwang, P. Sikivie, D. B. Tanner, R. Bradley, and J. Clarke, *Phys. Rev. Lett.* **104**, 041301 (2010).
- [21] J. Hoskins, J. Hwang, C. Martin, P. Sikivie, N. S. Sullivan, D. B. Tanner, M. Hotz, L. J. Rosenberg, G. Rybka, A. Wagner, S. J. Asztalos, G. Carosi, C. Hagmann, D. Kinion, K. van Bibber, R. Bradley, and J. Clarke, *Phys. Rev. D* **84**, 121302 (2011).
- [22] A. Caldwell, G. Dvali, B. Majorovits, A. Millar, G. Raffelt, J. Redondo, O. Reimann, F. Simon, and F. Steffen (MADMAX Working Group), *Phys. Rev. Lett.* **118**, 091801 (2017).
- [23] B. M. Brubaker, L. Zhong, Y. V. Gurevich, S. B. Cahn, S. K. Lamoreaux, M. Simanovskaia, J. R. Root, S. M. Lewis, S. Al Kenany, K. M. Backes, I. Urdinaran, N. M. Rapidis, T. M. Shokair, K. A. van Bibber, D. A. Palken, M. Malnou, W. F. Kindel, M. A. Anil, K. W. Lehnert, and G. Carosi, *Phys. Rev. Lett.* **118**, 061302 (2017).
- [24] W. Chung, *Proceedings, 15th Hellenic School and Workshops on Elementary Particle Physics and Gravity (CORFU2015): Corfu, Greece, September 1-25, 2015*, PoS **CORFU2015**, 047 (2016).
- [25] B. T. McAllister, G. Flower, E. N. Ivanov, M. Goryachev, J. Bourhill, and M. E. Tobar, *Physics of the Dark Universe* **18**, 67 (2017).
- [26] Y. Kahn, B. R. Safdi, and J. Thaler, *Phys. Rev. Lett.* **117**, 141801 (2016), arXiv:1602.01086 [hep-ph].
- [27] B. T. McAllister, G. Flower, L. E. Tobar, and M. E. Tobar, *Phys. Rev. Applied* **9**, 014028 (2018).
- [28] P. Sikivie, N. Sullivan, and D. B. Tanner, *Phys. Rev. Lett.* **112**, 131301 (2014).
- [29] B. T. McAllister, S. R. Parker, and M. E. Tobar, *Phys. Rev. D* **94**, 042001 (2016), arXiv:1605.05427 [physics.ins-det].
- [30] O. Reimann, “A novel microwave axion-detector,” (2016), “Detectors And Instrumentation Workshop”, Max-Planck-Institut für Physik.
- [31] B. T. McAllister, S. R. Parker, and M. E. Tobar, *Phys. Rev. Lett.* **116**, 161804 (2016), [Erratum: *Phys. Rev. Lett.* **117**, no.15, 159901 (2016)], arXiv:1607.01928 [hep-ph].
- [32] E. J. Daw, *A search for halo axions*, Ph.D. thesis, MIT (1998).
- [33] M. Goryachev, E. N. Ivanov, F. van Kann, S. Galliou, and M. E. Tobar, *Applied Physics Letters* **105**, 153505 (2014), <https://doi.org/10.1063/1.4898813>.
- [34] *HFC 50 D / E Dual Cryogenic Ultra Low Noise RF-Amplifier*, Stahl Electronics (2016), version 2.38.

### Details of Current and Voltage Derivation

We begin with the electric and magnetic fields induced by axions inside a uniform z-direction magnetic field.

$$\begin{aligned}\vec{E}_a &= E_a \hat{z} = \frac{1}{\epsilon_r} g_{a\gamma\gamma} c B_0 a \hat{z} \\ \vec{B}_a &= \mu_r \frac{1}{2} \frac{g_{a\gamma\gamma}}{c} r B_0 \frac{\partial a}{\partial t} \hat{\phi}.\end{aligned}$$

Here  $r$  is the distance from the centre of the solenoid, and  $\hat{z}$  and  $\hat{\phi}$  are the z-direction and  $\phi$ -direction unit vectors in the cylindrical co-ordinate system of the solenoid.

In this section we consider the signal from a parallel plate capacitor embedded in the magnetic field, such that the vector area of the plates are aligned with the induced electric field. The capacitance of a parallel plate capacitor with plate area  $A$  and separation  $d$  is given by  $C = \frac{\epsilon_0 \epsilon_r A}{d}$ . The voltage across the plates as a result of the axion induced electric field,  $\vec{E}_a$  is given by

$$\begin{aligned}V &= \int_0^d E_a dz \\ &= \frac{1}{\epsilon_r} g_{a\gamma\gamma} c B_0 a d,\end{aligned}$$

where  $a = a_0 \cos(\omega_a t)$ . Now

$$\begin{aligned}I &= C \frac{dV}{dt} \\ &= -C \frac{\omega_a}{\epsilon_r} g_{a\gamma\gamma} c B_0 d a_0 \sin(\omega_a t) \\ &= -A \epsilon_0 \omega_a g_{a\gamma\gamma} c B_0 a_0 \sin(\omega_a t).\end{aligned}$$

Where we have used  $C = \frac{\epsilon_0 \epsilon_r A}{d}$ . It can be shown that

$$a_0 = \sqrt{\frac{2\rho_a}{c} \frac{\hbar}{m_a}} \quad [32], \text{ so}$$

$$\begin{aligned}I_a(t) &= -g_{a\gamma\gamma} \epsilon_0 A B_0 \sqrt{2\rho_a c^5} \sin(\omega_a t) \\ V_a(t) &= \frac{1}{\epsilon_r} g_{a\gamma\gamma} B_0 \sqrt{2\rho_a c} \frac{\hbar}{m_a} d \cos(\omega_a t),\end{aligned}$$

or, for the RMS values

$$\begin{aligned}I_{a_{RMS}} &= -g_{a\gamma\gamma} \epsilon_0 A B_0 \sqrt{\rho_a c^5} \\ V_{a_{RMS}} &= \frac{1}{\epsilon_r} g_{a\gamma\gamma} B_0 \sqrt{\rho_a c^5} \frac{1}{\omega_a} d.\end{aligned}$$

### Details of Input Voltage Noise of High-impedance amplifier

In considering the effective voltage noise of the amplifier, referred to the input ( $\delta u_{eff}$ ) we must consider contributions as a result of the input voltage noise ( $\delta u_V$ ), the input current noise ( $\delta u_I$ ), and the thermal input noise ( $\delta u_{Th}$ ). This can be presented as,

$$\delta u_{eff} = \sqrt{\delta u_V^2 + \delta u_I^2 + \delta u_{Th}^2}.$$

We will now discuss each of these quantities.  $\delta u_I$  and  $\delta u_{Th}$  must be found via,

$$\begin{aligned}\delta u_I &= \delta i_{amp} \times |Z|, \\ \delta u_{Th} &= \delta i_{Th} \times |Z|.\end{aligned}$$

Here  $\delta i_{amp}$  is in the intrinsic amplifier current noise and  $\delta i_{Th}$  is the thermally induced current noise given by

$$\delta i_{Th} = \sqrt{\frac{k_B T_0}{R_{amp}}},$$

where  $k_B$  is the Boltzmann constant,  $T$  is the physical temperature, and  $R_{amp}$  is the amplifier input resistance, and finally  $Z$  is the complex impedance of the amplifier and capacitor system given by

$$Z = \frac{R_{amp}}{1 + i2\pi f C R_{amp}},$$

where  $C$  takes into account the capacitance of the detector  $C_{det}$  and the input capacitance of the amplifier  $C_{amp}$  such that,

$$C = \frac{C_{det} C_{amp}}{C_{det} + C_{amp}}.$$

The final quantity,  $\delta u_V$  arises from the intrinsic amplifier input voltage noise  $\delta u_{amp}$  according to

$$\delta u_V = \delta u_{amp} \times \left| \frac{Z_{amp}}{Z_{amp} + Z_{det}} \right|.$$

Where  $Z_{amp}$  and  $Z_{det}$  are the amplifier and detector impedances given by

$$\begin{aligned}Z_{amp} &= \frac{R_{amp}}{1 + i2\pi f C_{amp} R_{amp}}, \\ Z_{det} &= \frac{1}{2\pi f C_{det}}.\end{aligned}$$

Taking the values for these equations from a suitable datasheet [34] and the detector parameters proposed in the main text, we arrive at a value for  $\delta u_{eff}$  which is roughly constant as a function of frequency, at  $\delta u_{eff} \approx 1 \times 10^{-7} \frac{V}{\sqrt{Hz}}$  from 1 kHz to 1 MHz. This will be heavily dependent on the specific parameters of the amplifier and detector, but for the purposes of these sensitivity estimates this is the value we employ.